Bull. Chem. Soc. Jpn., 70, 2279—2286 (1997)

Linear and Stack Oligostreptocyanines. Effects of Relative Orientation of Chromophores on Redox Potentials of Dye Aggregates

Takashi Katoh, Yoshio Inagaki, and Renji Okazaki*,†

Ashigara Research Laboratories, Fuji Photo Film Co., Ltd., 210 Nakanuma, Minami-ashigara, Kanagawa 250-01

†Department of Chemistry, Graduate School of Science, The University of Tokyo, 7-3-1 Hongo, Bunkyo-ku, Tokyo 113

(Received April 16, 1997)

Linear and stack pentamethinestreptocyanine oligomers were prepared in which streptocyanines are covalently connected to each other. The absorption bands of the linear oligomers showed bathochromic shifts compared to that of the corresponding monomer, while the absorption band of the stack dimer was hypsochromically shifted. These spectral shifts were reproduced by a calculation with the INDO/S-CI method and are in agreement with those based upon a molecular exciton theory. The redox potentials of the linear oligomers underwent a positive shift due to the Coulombic interaction compared to those of the streptocyanine monomer. The positive shift of the reduction potential and the negative shift of the oxidation potential of the stack dimer are explained in terms of the Coulombic and orbital interactions.

Although aggregates of polymethine dyes are well-known and widely used as spectral sensitizers of photographic materials,[1] the properties of polymethine dye aggregates still remain ambiguous. Usually, a bathochromically-shifted band is called a *J*-band (*J* for Jelly, one of the first workers who investigated these shifts), while a hypsochromically-shifted one is called an *H*-band (*H* for hypsochromic).[2]

The relationship between the relative orientation of chromophores and the spectral shifts of a dye aggregate has been explained in terms of molecular exciton theory.[3] In the molecular exciton theory, a dye molecule is regarded as a point dipole and the excited state of a dye aggregate splits into two levels through interaction of transition dipoles (Fig. 1). In a parallel dimer with a large slip angle (α), a transition to the upper state of the two excited states is allowed and hence the absorption of a dimer is hypsochromically shifted compared to the corresponding monomer. On the other hand, in a head-to-tail dimer with a small slip angle (α), a transition to the lower state is allowed and hence the absorption undergoes a bathochromic shift.

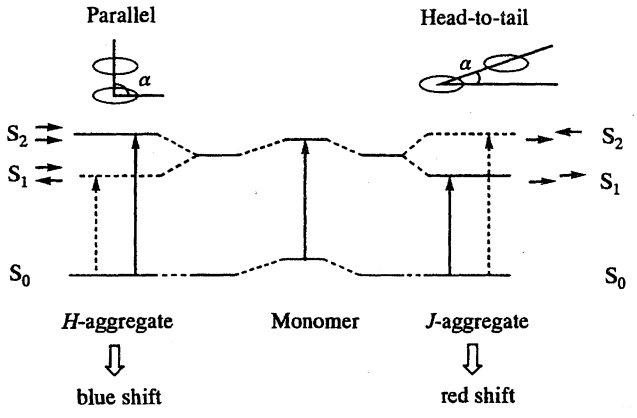

Fig. 1. Schematic diagram of the relationship between chromophore arrangements and spectral shifts based on the molecular exciton theory.

Molecular exciton theory can predict spectral shifts of a dye aggregate. However, it is probably unsuitable for prediction of orbital energy levels of a dye aggregate, since the molecular exciton theory is valid only when the interaction between orbitals of constituent molecules is negligible. The effect of chromophore arrangements on the orbital energy levels of aggregates has rarely been demonstrated. This is probably due to the experimental difficulty in preparing a dye aggregate in which a mode of the chromophore arrangement and the number of constituent molecules are well defined.

In order to clarify the property of polymethine dye aggregates, some attempts have been carried out to synthesize model compounds in which more than two chromophores were covalently linked, but compounds suitable for *H*- and *J*-aggregate models have not yet been prepared. Nakanishi et al. synthesized a bis-streptocyanine with a 1,2-cyclohexane linkage for which a molecular mechanical calculation suggested that a V-shaped configuration at the angle of ca. 70° is the most stable.[4] The splitting of an absorption band in solution was explained in terms of molecular exciton theory. However, the instability of the bis-streptocyanine in solution made it difficult to investigate the fluorescence and redox potentials. In order to overcome this problem, pentamethinestreptocyanines which are more stable than heptamethinestreptocyanines, were selected, and a linear dimer (**1a**), a trimer (**1b**), and a stack dimer (**2**) were designed (Chart 1) (compounds in which two or three chromophores are linked are called a dimer and a trimer, respectively, in this paper). The nitrogen atoms of two chromophores in **1a**

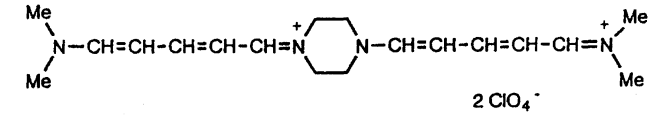

1a

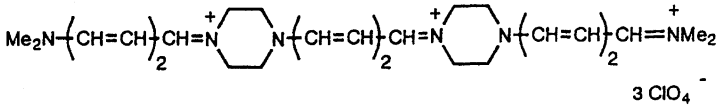

1b

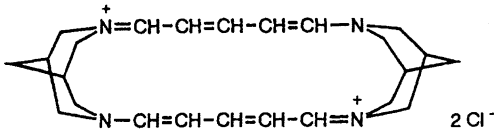

2

Chart 1.

and **2** are mutually linked by two ethylene and substituted trimethylene chains to fix the chromophore arrangements.

In this paper, the syntheses, absorption and fluorescence spectra, and redox potentials of the linear and stack streptocyanine oligomers are described.

Results and Discussion

Synthesis. The linear dimer **1a** was prepared by an acid-catalyzed condensation reaction between piperazine and unsaturated aldehyde **4** in 70% yield (Scheme 1). A linear trimer **1b** was prepared via an unsymmetrical streptocyanine **5** where one nitrogen atom of the piperazine ring was pro-

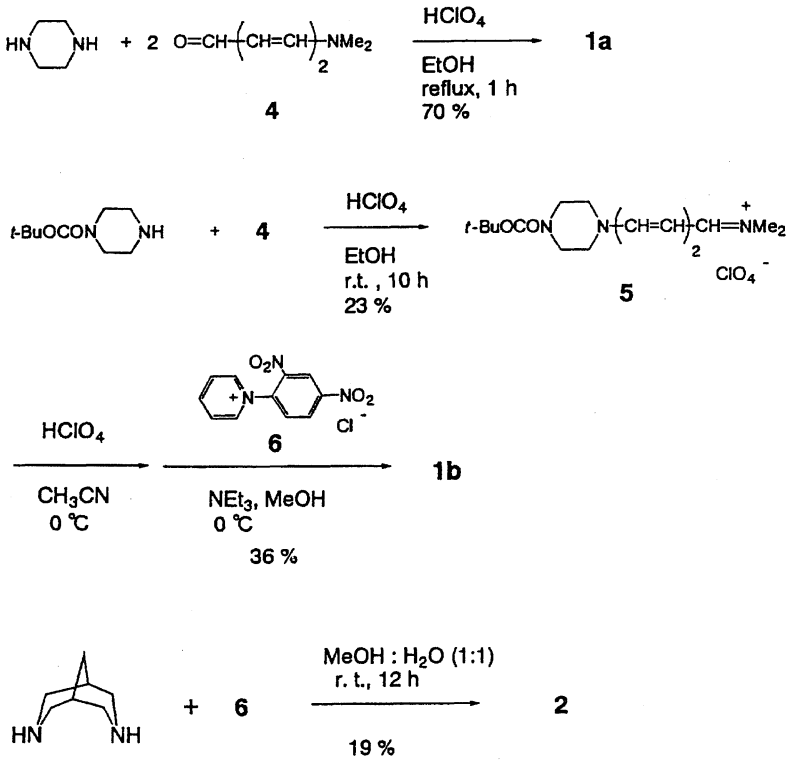

Scheme 1.

tected by a *t*-butoxycarbonyl (*t*-boc) group. After the deprotection of the *t*-boc group of **5** by aqueous perchloric acid, a condensation reaction with 1-(2,4-dinitrophenyl)pyridinium chloride (**6**) afforded **1b** in 36% yield (Scheme 1). The stack dimer **2** was prepared from bispidine (3,7-diazabicyclo[3.3.1]nonane) and **6** in aqueous solution in 19% yield (Scheme 1).

Structure. ^{1}H NMR spectrum of the linear dimer **1a** in acetone-d_6 at 296 K showed partly broadened peaks for the methine chain protons and that at 263 K showed two groups of sharp peaks for the methine chain protons, indicating that **1a** exists as a mixture of two isomers in solution. The coupling constants of the methine chain protons are within 12.0—13.0 Hz, confirming that methine chains of **1a** have all-*trans* conformation. The MM2 calculation[5] of **1a** gave two optimized structures, i.e., *trans* and *cis* conformers with respect to the orientation of the two streptocyanine moieties. The slip angles (α) of **1a** (*trans*) is 7.6° and the distances between the two center carbon atoms of the methine chains of **1a** (*trans*) and **1a** (*cis*) are 9.9 and 9.7 Å, respectively (Chart 2). ^{1}H NMR spectrum of the linear trimer **1b** in DMSO-d_6 at 298 K showed broadened peaks for the methine chain and piperazine ring protons. The MM2 calculation[5] of **1b** suggested that **1b** exists as a mixture of three isomers: i.e., *trans–trans*, *trans–cis*, and *cis–cis* conformers (Chart 3).

The ^{1}H NMR spectrum of the stack dimer **2** in DMSO-d_6 at 298 K showed sharp peaks due to only one isomer. The coupling constants (12.0—13.0 Hz) for the methine protons indicated an all-*trans* conformation of the methine chains. The optimized structure of **2** with the MM2 method[5] indicated a distance of 3.4 Å between the two center carbon atoms of the methine chains (Fig. 2).

The ^{1}H NMR spectra of **1a** and **2** showed the down-field shifts of methine protons compared to those of the monomer **3** (Fig. 3). These down-field shifts were attributed to the Coulombic effect of the neighboring cationic charge. The degree of the down-field shifts of **2** was larger than that

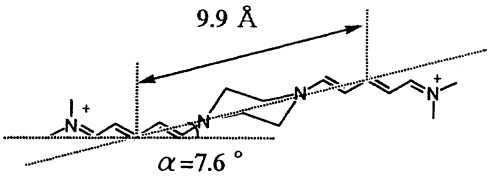

1a (*trans*)

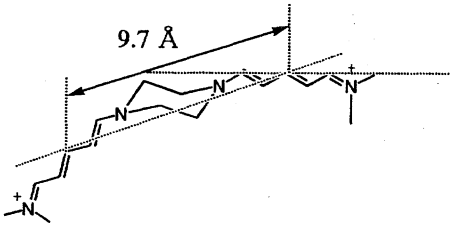

1a (*cis*)

Chart 2.

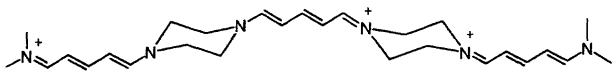

1b (*trans-trans*)

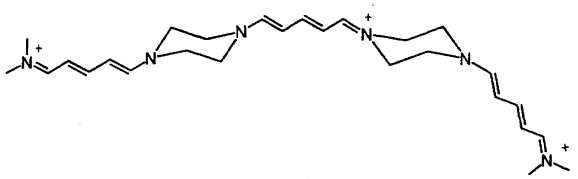

1b (*trans-cis*)

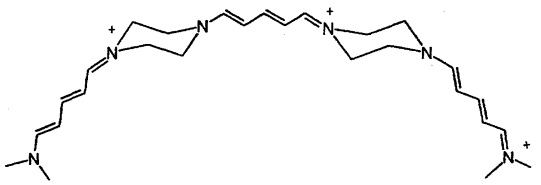

1b (*cis-cis*)

Chart 3.

(a)

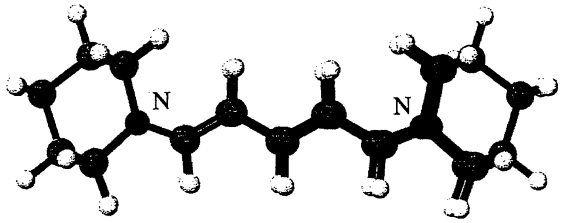

(b)

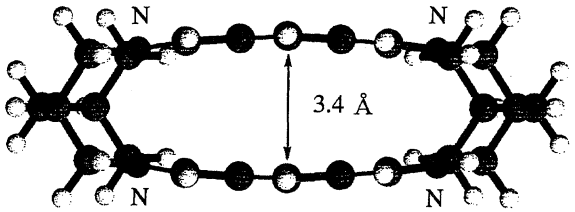

Fig. 2. The MM2 optimized structures of the stack dimer **2**; (a) the top view and (b) the side view.

of **1a**. This is explained by the difference in the distance between the two chromophores; the distance between the two center carbon atoms of the methine chains of **2** (3.4 Å) is shorter than that of **1a** (ca. 10 Å).

Absorption Spectra. The absorption spectra of **1a** and

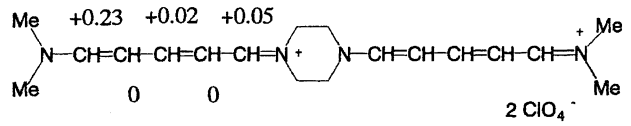

1a

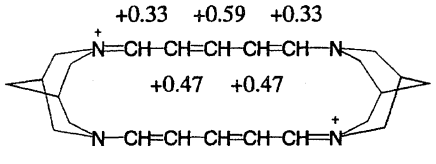

2

Fig. 3. The down-field shifts for the methine protons of the linear dimer **1a** and the stack dimer **2** compared to the monomer **3** in DMSO-d_6 at 298 K.

1b in methanol showed 28 and 46 nm bathochromic shifts compared to that of the monomer **3**, respectively (Fig. 4a), while the absorption band of **2** in methanol underwent a hypsochromic shift of 40 nm compared to **3** (Fig. 4b). The extinction coefficients of the dimer **1a** and **2** are nearly twice that of the monomer **3** (Table 1).

When spectral shifts of dye aggregates are caused by interactions between transition dipoles, the shift energies (ΔE) are expected to be in proportion to $2\cos(\pi/(n+1))$ (n is the number of chromophores in an aggregate).[6] Maruyama and Osuka reported that the absorption bands of linear and stack porphyrin oligomers connected by aromatic spacers afforded linear relationships between the shift energies and $2\cos(\pi/(n+1))$.[7] In the linear oligomers, **1a** and **1b**, the linear correlation between the shift energies (ΔE) and $2\cos(\pi/(n+1))$ ($n=2$ for **1a**, $n=3$ for **1b**) were actually found, indicating the presence of exciton couplings (Fig. 5).

Molecular Orbital Calculations. The molecular structures for **1a** and **2**, omitting counter anions, were optimized with the MM2 method.[5] The orbital energy levels of both **1a** and **2** calculated with the INDO/S-CI method[8] are lower than those of the corresponding monomer **3**, and the highest occupied molecular orbital (HOMO) and lowest unoccupied molecular orbital (LUMO) levels are no longer degenerate due to the orbital interactions (Fig. 6). The phase relationship of **2** is represented in Fig. 6. The degree of splittings of the orbital energy levels of **2** is larger than that of **1a**.

The electronic absorption bands of **1a** (*trans* and *cis*) and **2** calculated with the INDO/S-CI method[8] reproduced bathochromic shifts for **1a** (*trans* and *cis*) and a hypsochromic shift for **2** compared to the monomer **3** (Table 1). The absorption bands of **1a** (*trans*) consist of an intense one at 415 nm ($f=2.28$, f is oscillator strength) and a weak one at 373 nm ($f=0.005$). Similarly, **1a** (*cis*) has two absorption bands at 418 nm ($f=2.30$) and at 373 nm ($f=0.45$). The bathochromic and hypsochromic absorption bands of **1a** (*cis*) correspond to the theoretically allowed transition to the lower excited state and the forbidden transition to the upper excited state, respectively. The hypsochromic absorption band around 385 nm of **1a** in methanol (Fig. 4a) can be interpreted as a hypsochromic absorption band of the *cis* conformer. The degree of splittings of excited states of **1a** is estimated to be ca. 3140 cm^{-1} from the separation of the two absorption peaks in methanol. These calculations reproduced the observed absorption spectrum of **1a** in methanol.

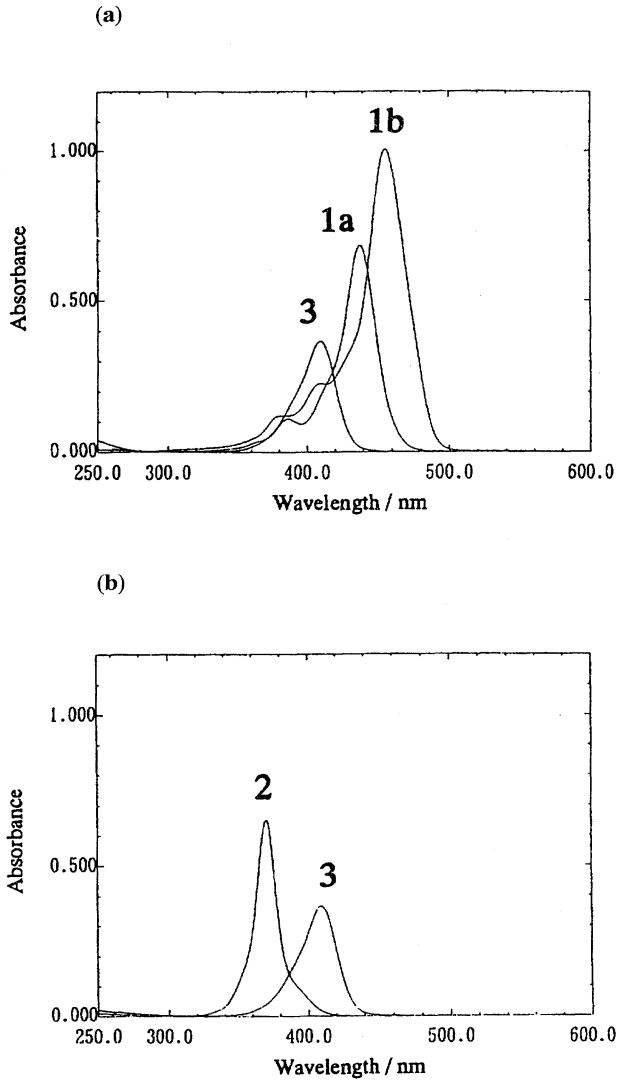

Fig. 4. Absorption spectra in methanol at 298 K (0.33×10^{-5} mol dm^{-3}) of (a) the linear dimer **1a** and the trimer **1b**, and (b) the stack dimer **2**.

On the other hand, the absorption bands of the stack dimer **2** consist of a weak one at 393 nm ($f=0.60$) and an intense one at 333 nm ($f=2.35$).

Interactions between chromophores in multichromophoric compounds are mainly classified into through-space and through-bond interactions. Paddon-Row et al. emphasized the through-bond effect as well as through-space effect on excitonic interactions in rigidly linked dinaphthyl molecules.[9] A hypothetical streptocyanine dimer in which the two cyanine parts are not bound covalently is a good model to estimate the through-space and through-bond interaction separately. At first, we chose the hypothetical dimer **7** (Chart 4) in which the arrangement of two cyanine moieties is identical

Table 1. Observed and Calculated Absorption Spectra of the Linear Dimer **1a** (*trans* and *cis*), the Stack Dimer **2** and the Hypothetical Stack Dimer **9**

Compounds	Observed[a]		Calculated[b]		
	λ_{max}/nm	$\varepsilon(10^5)$[c]	λ_{max}/nm	f[d]	Transition character[e]
1a(*trans*)	438	2.1	415	2.71	0.71(H→L)+0.67(H−1→L+1)
			373	0.005	0.70(H→L+1)+0.67(H−1→L)
1a(*cis*)	438	2.1	418	2.30	0.71(H→L)+0.67(H−1→L+1)
			373	0.45	0.70(H→L+1)+0.67(H−1→L)
2	370	2.1	393	0.60	0.96(H→L+1)
			333	2.35	0.96(H−1→L+1)
9	—	—	412	0.60	0.94(H→L+1)
			335	2.12	0.94(H−1→L+1)
3	410	1.1	390	1.21	0.98(H→L)

a) In methanol at 298 K. b) The MM2 optimized structures without counter anions were used. The absorptions were calculated with the INDO/S-CI method. c) Extinction coefficients. d) Oscillator strengths. e) H and L stand for HOMO and LUMO, respectively.

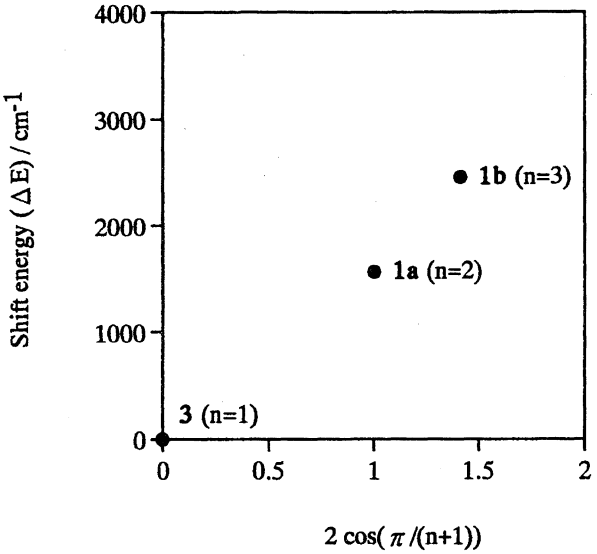

Fig. 5. Relationship between the spectral shift energies (ΔE) and 2 cos ($\pi/(n+1)$) in the linear oligomers **1a** ($n=2$) and **1b** ($n=3$).

with that in **1a** (*trans*). This model structure, suffering from severe steric congestion around the closely placed dimethylamino groups, gave apparently unusual orbital energy levels and absorption bands by the INDO/S-CI calculation. We, therefore, employed another strategy in which two streptocyanine molecules are gradually brought closer together while changing the intermolecular distance, R, from 14.2 to 11.2 Å (**8**, Chart 4). Figure 7 shows the dependence of the distance, R, on the shift energies calculated with the INDO/S-CI method compared to the monomer **3**. From this relationship, through-space interaction of **1a** ($R=9.9$ Å) is estimated to be 1580 cm^{-1}, which is nearly equal to the observed shift energy (1540 cm^{-1}) of **1a** in methanol. Accordingly, the exciton coupling of **1a** is considered to be mainly due to a through-space interaction.

The hypsochromic shift of the hypothetical stack dimer **9** compared to the monomer **3** is nearly equal to that of the stack dimer **2** (Table 1), indicating the absence of a through-bond exciton coupling in the stack dimer linked via a bispidine skeleton.

Fluorescence Spectra. Fluorescence spectra of **1a**, **1b**, and **2** in methanol at 298 K revealed that the linear oligomers **1a** and **1b** had larger fluorescence intensities and smaller Stokes shifts than those of **3**, while the stack dimer **2** had a smaller fluorescence intensity and a larger Stokes shift than those of **3** (Table 2). These observations can be explained in terms of the molecular exciton theory, which predicts large Stokes shifts and weak fluorescences for *H*-aggregates due to the internal conversion from the upper excited states to lower ones and the forbidden transitions from the lower excited states.

Redox Potentials. Redox potentials of the linear oligomers, **1a** and **1b**, and the stack dimer **2** were measured by polarography (Table 3). The polarogram of **1a** indicated one-stage two-electron oxidation and reduction processes. The reduction and oxidation potentials for the linear oligomers **1a** and **1b** were positively shifted compared to those for the monomer **3**. On the other hand, the polarogram of the stack dimer **2** showed two oxidation waves and two one-electron reduction waves. The reduction potential of **2** was 0.19 V positively shifted compared to that of the monomer **3**, while the first oxidation potential of **2** was 0.22 V negatively shifted.

The appearance of two reduction waves is probably due to the decrease of the Coulombic interactions after one-electron reduction (Fig. 8). Namely, Coulombic interaction between an electron and the cyanine cation is larger than that between an electron and an uncharged radical in the reduced cyanine. Similarly, the two oxidation waves could be considered to be due to Coulombic interactions. The oxidation wave at 1.05

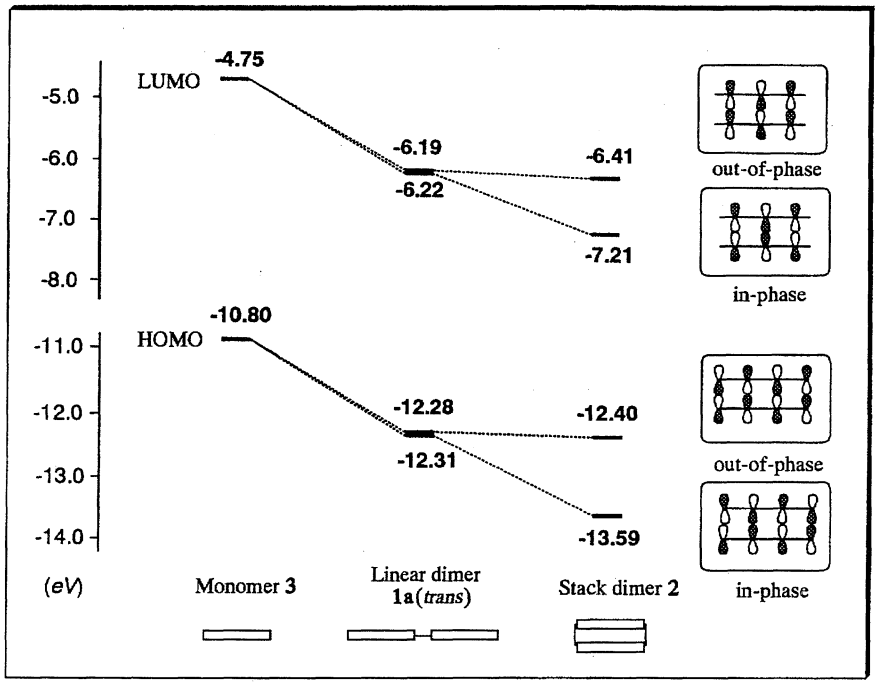

Fig. 6. Orbital energy levels of the linear dimer **1a** (*trans*) and the stack dimer **2** calculated with the INDO/S-CI method. The phase relationship of **2** is represented in square frames.

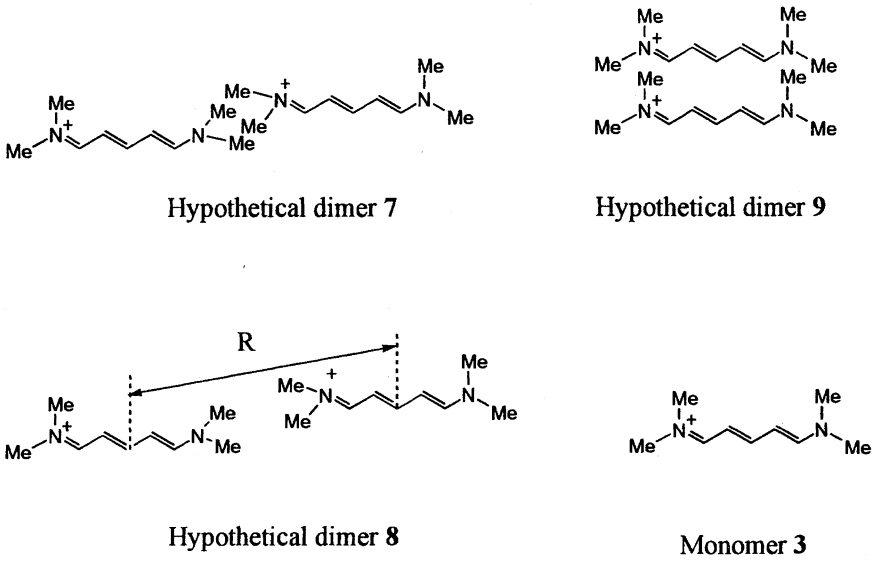

Chart 4.

V, however, is overlapped with that for the chloride ion of **2**, and Coulombic interactions during the oxidation process could not be investigated.

The oxidation and reduction potentials of polymethine dyes correlate to the HOMO and LUMO energy levels, respectively. Based upon the results of these redox potentials, we propose that the orbital energy levels (E_{aggr}) of polymethine dye aggregates are represented by those of monomers (E_{mono}), the charge interaction (E_{cha}), and the orbital interaction (E_{orb}) (Eq. 1).

$$E_{aggr} = E_{mono} + E_{cha} + E_{orb} \quad (1)$$

The charge interaction (E_{cha}) is Coulombic attraction between the cationic charge of the neighboring cyanine and electrons, causing the positive shifts of both reduction and oxidation potentials.

Since the orbital interaction of the linear dimer **1a** is negligible, the positive shifts in redox potentials of **1a** compared to those of the monomer **3** are considered to be due to the charge interaction, which corresponds to be +0.11 V for the oxidation potential and +0.05 V for the reduction potential.

When dye molecules aggregate, the orbital overlaps between chromophores cause a change in the orbital energy levels. Since the HOMO and LUMO of a stack dimer are derived from the *anti*-bonding and bonding combinations (Fig. 6), the orbital interactions (E_{orb}) make the reduction and oxidation potentials more positively and negatively shifted,

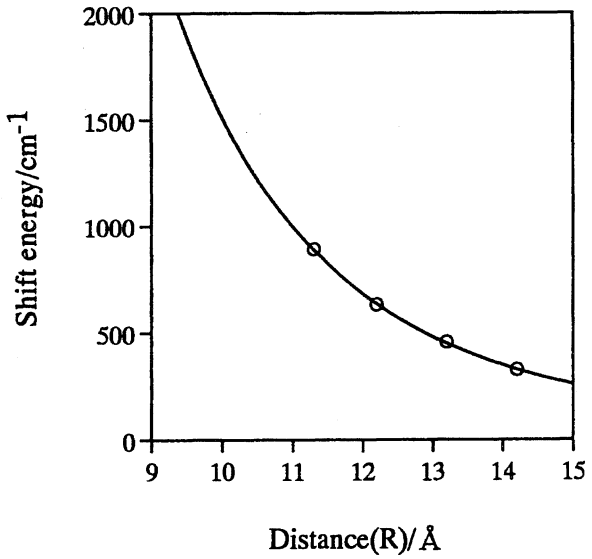

Fig. 7. The relationship between the shift energy calculated with the INDO/S-CI method and the distance (R) of the two center carbon atoms of the methine chains in the hypothetical linear dimer **8**.

Table 2. Fluorescence Maxima, Relative Intensities, and Stokes Shifts of the Linear Dimer **1a**, the Linear Trimer **1b**, and the Stack Dimer **2**

Compounds	Absorption[a]	Fluorescence[a]		
	λ_{max}/nm	λ_{max}/nm	Relative intensity	Stokes shifts cm^{-1}
1a	438	460	2.95	1090
1b	456[b]	484[b]	1.45[b]	1250[b]
2	370	415	0.014	2930
3	410	440	1.0 (standard)	1670
	410[b]	440[b]	0.98[b]	1670[b]

a) In methanol at 298 K. b) In acetonitrile at 298 K.

Table 3. Redox Potentials of the Linear Dimer **1a**, the Linear Trimer **1b**, the Stack Dimer **2**, and the Monomer **3** Measured with Polarography

Compounds	E_{ox} (V vs. SCE)[a]	E_{red} (V vs. SCE)[b]
1a	1.09	−1.31
1b	1.13	−1.19
2	0.76, 1.05	−1.17, −1.38
3	0.98	−1.36

a) Oxidation potentials in CH_3CN containing 0.1 M $NaClO_4$.
b) Reduction potentials in CH_3CN containing 0.1 M n-Pr_4NClO_4.

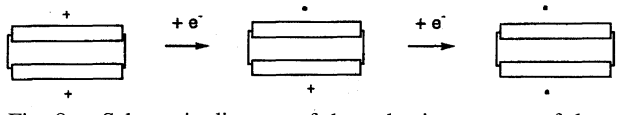

Fig. 8. Schematic diagram of the reduction process of the stack dimer **2**.

respectively. The negative shifts of the oxidation potential of the stack dimer **2** compared to that of the monomer **3** indicated that the orbital interaction of **2** is larger than the charge interaction. The positive shift of the reduction potential of **2** is considered to be based on both the orbital and charge interactions.

It is noteworthy that the relative orientation of streptocyanine chromophores has a pronounced effect on energy levels of dye aggregates, in view of the molecular exciton theory which assumes the difference of energy levels between dye aggregates and the monomer to be negligible.

Conclusion. Streptocyanine oligomers in which streptocyanines are covalently connected to each other in linear and stack modes were prepared. The spectral shifts were in agreement with those based upon the molecular exciton theory. The redox potentials of the linear oligomers positively shifted compared to those of the monomer due to Coulombic interactions. The shifts of the redox potentials of the stack dimer were explained by both the Coulombic and orbital interactions. The relative orientation of chromophores affects not only energy levels of dye aggregates but also transition energies of aggregate bands.

Experimental

Melting points were uncorrected. ^1H NMR spectra were determined on a Bruker ARX-300 (300 MHz) spectrometer and chemical shifts are quoted in ppm downfield from $SiMe_4$. Infrared spectra were recorded using a JASCO IR-810 spectrometer. UV/vis spectra were recorded on a Shimadzu UV-3100PC spectrometer. Fluorescent spectra were obtained on a Hitachi 850 fluorescence spectrophotometer. Relative intensities were calculated based upon the optical densities at the fluorescent maxima; monomer **3** was used as a reference. FAB-mass spectra were measured by a JEOL DX-303 mass spectrometer. Redox potential measurements were carried out on a Yanaco polarographic analyzer P-1100. Reduction potentials were measured with a dropping mercury working electrode with a saturated calomel electrode (SCE) as a reference electrode in CH_3CN with 0.1 M $NaClO_4$ (1 M=1 mol dm^{-3}). Oxidation potentials were measured with a rotating Pt working electrode and SCE as a reference electrode in CH_3CN with 0.1 M n-Pr_4NClO_4. Acetonitrile for electrochemistry was dried over molecular sieves 4 Å. Sephadex LH-20 (Pharmacia Biotech) was used.

All MO calculations were performed on a SONY Tektronix CAChe system. Molecular structures were optimized with an MM2 method.[5] The electronic spectra were calculated with an INDO/S-CI method[8] considering 20 configuration interaction levels.

5-(*N,N*-Dimethylamino)-2,4-pentadienal (**4**),[10] bispidine,[11] and 5-dimethylamino-2,4-pentadienylideneammonium perchlorate (**3**)[10] were prepared by the literature procedures. All solvents and other materials were of commercial grade and were used without further purification.

Caution: perchlorate compounds are explosive and should be handle carefully.

Preparation of 1-(5-Dimethylamino-2,4-pentadienylidene)-4-[5-(dimethylimmonio)-1,3-pentadienyl]-1-piperazinium Diperchlorate (1a). To an ethanol solution (10 ml) of 5-dimethylamino-2,4-pentadienal (**4**) (1.25 g, 10 mmol) and piperazine (0.40 g, 4.65 mmol) was added 70% aqueous perchloric acid (0.80 ml), and the solution was stirred for 30 min at 60 °C. After cooling, the precipitates were filtered and washed with acetone. The crude products were dissolved in DMSO (2 ml) and to this solution was added acetonitrile (20 ml). The precipitates were filtered off, washed with acetone, and dried to afford **1a** as yellow crystals (0.32 g, 26%); mp

273—278 °C (decomp); UV/vis (MeOH) λ_{max} 438 nm (ε=210000); ^{1}H NMR (DMSO-d_6, 298 K) δ=3.11 (s, 6H), 3.38 (s, 6H), 3.6—3.9 (b, 8H), 5.8—6.0 (b, 4H), 7.48 (t, 2H, J=13 Hz), 7.7 (b, 2H), 7.9 (d, 2H J=13 Hz); IR (KBr) 1550, 1450, 1404, 1180, 1120, 1004, 860 cm^{-1}; MS (FAB) m/z 401 (M−ClO_4). Found: C, 42.27; H, 5.88; N, 10.76%. Calcd for $C_{18}H_{30}Cl_2N_4O_8 \cdot 0.5H_2O$: C, 42.36; H, 6.12; N, 10.98%.

Preparation of 5-[4-(*t*-Butoxycarbonyl)-1-piperazinyl]-2,4-pentadienylidenedimethylammonium Perchlorate (5). To an ethanol solution (10 ml) of **4** (0.41 g, 3.3 mmol) and 1-*t*-butoxycarbonylpiperazine (0.62 g, 3.3 mmol) was added 70% aqueous perchloric acid at room temperature. Purification by Sephadex column chromatography using methanol afforded **5** as yellow crystals (0.32 g, 26%); mp 160—165 °C (decomp); UV/vis (MeOH) λ_{max} 414 nm (ε=109000); ^{1}H NMR ($CDCl_3$) δ=1.55 (s, 9H), 3.10 (s, 3H), 3.32 (s, 3H), 3.4—3.6 (b, 8H), 5.6—5.8 (b, 2H), 7.7—7.9 (b, 3H); IR (KBr) 1700, 1570, 1410, 1205, 1170, 1092, 1018, 850, 620 cm^{-1}; MS (FAB) m/z 294 (M−ClO_4^-).

Preparation of 5-(4-Azonia-{5-[4-azonia-4-(5-dimethylamino-2,4-pentadienylidene)piperidino]-2,4-pentadienylidene}piperidino)-2,4-pentadienylidenedimethylammonium Triperchlorate (1b). To an acetonitrile solution (5 ml) of **5** (135 mg, 0.34 mmol) was added aqueous perchloric acid (50 mg, 3.5 mmol) at 0 °C. After the solution was stirred for 0.5 h at 0 °C, 1-(2,4-dinitrophenyl)pyridinium chloride (**6**) (39 mg, 0.14 mmol) and then an acetonitrile solution (2 ml) of triethylamine (40 mg, 0.4 mmol) and methanol (0.04 ml) were added and the solution was stirred for 1 h. After addition of methanol, the precipitates were filtered off. Recrystallization from methanol and dichloromethane afforded **1b** as yellow crystals (37 mg, 36%); mp 210—220 °C (decomp); UV/vis (MeOH) λ_{max} 456 nm (ε=300000); ^{1}H NMR (DMSO-d_6, 298 K) δ=3.08 (s, 6H), 3.30 (s, 6H), 3.7—3.9 (b, 16H), 5.8—6.1 (m, 6H), 7.4—7.6 (m, 3H), 7.7—8.0 (m, 6H); IR (KBr) 1540, 1440, 1360, 1170 cm^{-1}; MS(FAB) m/z 649 (M−ClO_4^-). Found: C, 42.89; H, 5.58; N, 10.76%. Calcd for $C_{18}H_{30}Cl_3N_6O_{12} \cdot 0.5H_2O$: C, 42.72; H, 5.84; N, 11.07%.

Preparation of 7,19-Diaza-1,13-diazoniapentacyclo[19.3.1.1^{7,11}.1^{9,13}.1^{19,23}]octacosa-1,3,5,13,15,17-hexaene Dichlorate (2). To an 50% aqueous methanol solution (40 ml) of **6** (140 mg, 0.50 mmol) was added bispidine (65 mg, 0.51 mmol) at 25 °C and the reaction solution was stirred for 12 h at 25 °C. Repeated purification by Sephadex column chromatography using methanol afforded **2** as pale yellow crystals (27 mg, 0.095 mmol, 19%); mp 285—295 °C (decomp); UV/vis (DMSO) λ_{max} 370 nm (ε=210000); ^{1}H NMR (DMSO-d_6, 298 K) δ=1.95−2.0 (m, 2H), 2.05—2.15 (m, 2H), 3.45 (d, 4H, J=14 Hz), 3.80 (d, 4H, J=14 Hz), 4.20 (d, 4H, J=14 Hz), 4.48 (d, 4H, J=14 Hz), 6.32 (t, 4H, J=13 Hz), 7.95 (d, 4H, J=13 Hz), 8.07 (t, 4H, J=13 Hz); IR (KBr) 1600, 1450, 1230, 1074, 1018, 983 cm^{-1}; MS (FAB) m/z 412 (M−Cl^-). Found: C, 59.12; H, 7.58; N, 11.86%. Calcd for $C_{24}H_{34}Cl_2N_4 \cdot 2H_2O$: C, 59.38; H, 7.89; N, 11.54%.

References

1) D. Möbius, *Adv. Mater.*, **7**, 437 (1995); N. Tyutyulkov, J. Fabian, A. Mehlhorn, F. Dietz, and A. Tadjer, "Polymethine Dyes," St. Kliment Ohridski University Press, Sofia (1991); A. H. Herz, *Photogr. Sci. Eng.*, **18**, 323 (1974); T. Tani, "Photographic Sensitivity," Oxford University Press, New York (1995), Chap. 5, pp. 111—164; D. M. Sturmer and D. W. Heseltine, "The Theory of the Photographic Process," 4th ed, ed by T. H. James, McMillan Publ. Co., New York (1977), Chap. 8, pp. 194—234; P. B. Gilman, *Pure Appl. Chem.*, **49**, 357 (1977); W. West, *Photogr. Sci. Eng.*, **18**, 35 (1974).

2) E. E. Jelly, *Nature*, **138**, 1009 (1936); G. Scheibe, *Angew. Chem.*, **49**, 563 (1936).

3) E. G. McRae and M. Kasha, *J. Chem. Phys.*, **28**, 721 (1958); M. Kasha, H. R. Rawis, and M. A. El-Bayoumi, *Pure Appl. Chem.*, **11**, 371 (1965); G. S. Levinson, W. T. Simpson, and W. Curtius, *J. Am. Chem. Soc.*, **79**, 4314 (1957); K. Norland, A. Ames, and T. Taylor, *Photogr. Sci. Eng.*, **14**, 295 (1970).

4) N. Berova, D. Gargiulo, F. Derguini, K. Nakanishi, and N. Harada, *J. Am. Chem. Soc.*, **115**, 4769 (1993); D. Gargiulo, F. Derguini, N. Berova, K. Nakanishi, and N. Harada, *J. Am. Chem. Soc.*, **113**, 7046 (1991).

5) N. L. Allinger, *J. Am. Chem. Soc.*, **99**, 8127 (1977).

6) E. S. Emerson, M. A. Conlin, A. E. Rosenoff, K. S. Norland, H. Rodriguez, D. Chin, and G. R. Bird, *J. Phys. Chem.*, **71**, 2396 (1967).

7) K. Maruyama and A. Osuka, *Pure Appl. Chem.*, **62**, 1511 (1990).

8) J. Ridley and M. Zerner, *Theor. Chim. Acta (Berlin)*, **32**, 111 (1973).

9) G. D. Scholes, K. P. Ghiggino, A. M. Oliver, and M. N. Paddon-Row, *J. Am. Chem. Soc.*, **115**, 4345 (1993); K. D. Jordan and M. N. Paddon-Row, *Chem. Rev.*, **92**, 395 (1992).

10) S. S. Malhotra and M. C. Whiting, *J. Chem. Soc.*, **1960**, 3812.

11) H. Stetter and H. Hennig, *Chem. Ber.*, **88**, 789 (1955).